Rayleigh-Taylor instability in spherical geometry

N. K. Gupta and S. V. Lawande
Theoretical Physics Division, Bhabha Atomic Research Centre, Trombay, Bombay 400 085, India
(Received 5 April 1985; revised manuscript received 7 November 1985)

An analysis of the Rayleigh-Taylor instability in a spherical geometry is presented. Expanding any initial perturbation at a spherical surface between two fluids in spherical harmonics Y_{lm} and further assuming an exponential time growth of the expansion coefficients, an eigenvalue equation for the growth rate is obtained. The free-surface and jump boundary conditions are obtained from the eigenvalue equation. The eigenvalue equation is solved for solid spherical targets and analytical formulas for the growth rate of the instability are presented in the cases where the initial plasma density profile has a step function or exponential variation in space. An analytical expression for the growth rate is also presented for the shell targets and its variation with the aspect ratio of the shell is discussed.

The achievement of desired fusion yields in inertial confinement fusion (ICF) requires the compression of the fuel pellet to up to as high as 10^3 to 10^4 times the solid density. During the course of the spherical implosion that is required to achieve this high degree of compression[1] an unavoidable departure from symmetry arises. The main sources of these asymmetries are the pellet fabrication asymmetry, nonuniformity of driver beam illumination, and hydrodynamic instabilities. Among the hydrodynamic instabilities, the Rayleigh-Taylor instability[2] is an inherently unavoidable problem during the implosion of the ICF target. In the classical analysis[3] of semi-infinite, inviscid, incompressible fluids of constant density, the exponential growth rate γ of the instability is $(a_w Kg)^{1/2}$ where a_w is the Atwood number given by $(\rho_h-\rho_l)/(\rho_h+\rho_l)$, K is the wave number, and g is the acceleration, ρ_h and ρ_l being the densities of heavy and light fluids, respectively. In the case of a realistic ICF experiment, the analysis of the instability is complicated by the presence of density gradients, heat conduction, compressibility, flow of the ablating material, and spherical geometry. Recently a number of two- and three-dimensional numerical calculations[4–14] have been reported where all of these effects are taken into account, and the general prediction is a reduction of the growth rate by as much as a factor of 2 compared to the classical value. On the other hand, there have been some attempts to study a few of these effects analytically.[15–20] Most of this analytical work is restricted to a plane geometry. Some analysis of the fluid instability for a spherical geometry has been considered by Hunt[21] and Elliot[22]. Kidder[23] used his theory of homogeneous isentropic compression to predict the growth rate for spherical shell targets, and Book and Bernstein[24] have used self-similar solutions for the analysis of the instability in a spherical geometry. Recently, Takabe *et al.*[25] have developed a self-consistent analysis of the Rayleigh-Taylor instability in an ablating plasma, including the heat conduction and ablative flow.

In this paper we present our analysis of the instability in a spherical geometry. The initial disturbance at the density interface is expanded in spherical harmonics $Y_{lm}(\theta,\phi)$ and the expansion coefficients are assumed to grow exponentially with time. We derive an eigenvalue equation for the growth rate γ_{lm}, along with the different boundary conditions which are subsequently used to derive analytical formulas for solid and shell targets. In the analysis for the solid targets the initial density profile is assumed to be either a step function or an exponential in space. Incidentally, these two are the only density profiles which can be analyzed analytically. However, any realistic density profile that may exist in ICF experiments can always be approximated by a suitable combination of these two basic profiles. The analysis of this paper would therefore be relevant for treating a realistic density profile as well.

The dynamics of the imploding plasma is described by the hydrodynamic equations for an incompressible fluid

$$\frac{\partial\rho}{\partial t}+\nabla\cdot(\rho\mathbf{u})=0\ , \tag{1}$$

$$\rho\left[\frac{\partial\mathbf{u}}{\partial t}+(\mathbf{u}\cdot\nabla)\mathbf{u}\right]=-\nabla p+\mathbf{g}\rho\ , \tag{2}$$

$$\nabla\cdot\mathbf{u}=0\ , \tag{3}$$

where ρ and $\mathbf{u}$ are the density and velocity of the plasma, respectively, while p is the hydrodynamic pressure and $\mathbf{g}$ is the acceleration. The effects due to heat conduction and viscosity are neglected.

Assuming the fluid to be perturbed from its quiescent state, we replace ρ by $\rho_0+\delta\rho$ and p by $p_0+\delta p$ and linearize the above set of equations. For spherical geometry, the resulting set of equations involves ρ_0, $\delta\rho$, δp, the radial velocity u_r, and a quantity $D_1=\nabla_\perp\cdot\mathbf{u}_\perp$, $\mathbf{u}_\perp$ being the component of velocity in a direction normal to the radius vector. The next step is to expand the perturbed quantities $\delta\rho$, u_r , δp, and D_1 in terms of the spherical harmonics as

$$f(r,\theta,\phi,t)=\sum_{l,m} f_{lm}(r,t)Y_{lm}(\theta,\phi)\ , \tag{4}$$

where f stands for any of the perturbed quantities. The time dependence can be separated by making the customary assumption that

$$f_{lm}(r,t)=f_{lm}(r)e^{\gamma_{lm}t} . \quad (5)$$

Subsequently eliminating $(D_1)_{lm}$, $(\delta p)_{lm}$, and $(\delta\rho)_{lm}$ from the resulting set of equations, one can derive the equation determining the growth rate γ_{lm}:

$$\frac{d}{dr}\left[\rho_0(r)\frac{du_r}{dr}\right]+\frac{4\rho_0}{r}\frac{du_r}{dr}-\frac{l(l+1)}{r^2}\left[\frac{g}{\gamma^2}\frac{d\rho_0}{dr}+\rho_0\right]u_r + \frac{2\rho_0}{r^2}u_r+\frac{2}{r}\frac{d\rho_0}{dr}u_r=0 , \quad (6)$$

where for the simplicity of writing, we have suppressed the subscripts l,m. It is clear from Eq. (6) that the growth rate γ depends only on l and not on m. This degeneracy, with respect to m, has also been observed previously by many authors.[5,6,25] For a given density profile ρ_0 the growth rate γ is obtained by solving Eq. (6) under suitable boundary conditions. We note at first that u_r is finite as $r\to 0$ and vanishes as $r\to\infty$. Next, at a point of discontinuity in the plasma density (say at $r=R$) we require the jump condition [obtained by integrating Eq. (6) from $R-\epsilon$ to $R+\epsilon$ and letting $\epsilon\to 0$]

$$\Delta\left[\rho_0\frac{dur}{dr}\right]+\left[\frac{2}{R}-\frac{l(l+1)}{R^2}\frac{g}{\gamma^2}\right]u_r(R)\Delta(\rho_0)=0 , \quad (7)$$

where $\Delta(F)$ is defined as

$$\Delta(F)=F_{R+}-R_{R-} , \quad (8)$$

$F_{R+}(F_{R-})$ being the value of the function F just above (below) the point $r=R$. Finally, the boundary condition at a free surface $r=R$ [obtained by setting $\rho_0(R^+)$ or $\rho_0(R^-)=0$ in Eq. (7)] reads as

$$\left.\frac{du_r}{dr}\right|_R+\left[\frac{2}{R}-\frac{l(l+1)g}{R^2\gamma^2}\right]u_r(R)=0 . \quad (9)$$

We may also mention here that at a fixed boundary $u_r=0$. This condition is, however, not relevant in the cases presented in the paper.

We now consider some density profiles for ρ_0 leading to an analytical treatment of the problem. For solid spherical targets there are two cases of interest where analytical formulas for the growth rate γ can be derived from the solution of Eq. (6). The first case is that of a stepwise density profile

$$\rho_0(r)=\begin{cases}\rho_1 , & 0\le r\le R\\ \rho_2 , & R\le r<\infty\end{cases} \quad (10)$$

where the solution of Eq. (6), with appropriate boundary conditions, leads to the growth rate given by

$$\gamma^2=g(\rho_1-\rho_2)\frac{l(l+1)}{R}[\rho_1+l(\rho_1+\rho_2)]^{-1} . \quad (11)$$

Note in passing that for a sphere of radius R with a uniform density ρ_0 and a free surface at $r=R$, the growth rate γ is equal to $(lg/R)^{1/2}$. Comparing this result with the corresponding result in plane geometry, where $\gamma^2=Kg$, we may introduce an equivalent wave number for the spherical case by $K=l/R$. With this definition for K, comparing Eq. (11) with the corresponding plane case we may, for the purpose of subsequent discussion, introduce a parameter analogous to the Atwood number as

$$a_w^*=\frac{(l+1)(\rho_1-\rho_2)}{(l+1)\rho_1+l\rho_2} . \quad (12)$$

We also note that the large value of l implies a large value of K and hence this limit is equivalent to the short-wavelength limit of the plane case. Similarly $l=1$ (lowest permissible value of l) corresponds to the long wavelength limit of the plane case. Thus, in the following we will refer to the limits $l\gg 1$ and $l=1$ as, respectively, the "short wavelength" and "long wavelength" limits. In these two limits the quantity a_w^* takes the form

$$a_w^*=\begin{cases}(\rho_1-\rho_2)/(\rho_1+\rho_2) , & l\gg 1\\ (\rho_1-\rho_2)/(\rho_1+0.5\rho_2) , & l=1 .\end{cases} \quad (13)$$

Note that a_w^* for $l\gg 1$ is identical to the Atwood number for the plane geometry while for $l=1$ it is somewhat different.

The second case is that of a density profile with an exponential variation in r,

$$\rho_0(r)=Ae^{\beta r} , \quad 0\le r\le R , \quad (14)$$

where A and β are constants. The solution of Eq. (6) yields the normalized growth rate $\bar\gamma=\gamma/(Kg)^{1/2}$ $(K=l/R)$ given by

$$\bar\gamma^2=(l+1)\Big/\left[a-\frac{\beta R}{2}\frac{{}_1F_1(a+1,2a+1;-\beta r)}{{}_1F_1(a,2a;-\beta R)}\right] , \quad (15)$$

where ${}_1F_1(a,c;z)$ is the usual hypergeometric function[26] and the quantity a is defined as

$$a=0.5\left[1+\left[(2l+1)^2+\frac{4\beta R(l+1)}{\bar\gamma^2}\right]^{1/2}\right] . \quad (16)$$

We notice that $\bar\gamma^2$ depends on the product βR rather than individually on β and R. Also as the product $\beta R\to 0$, the

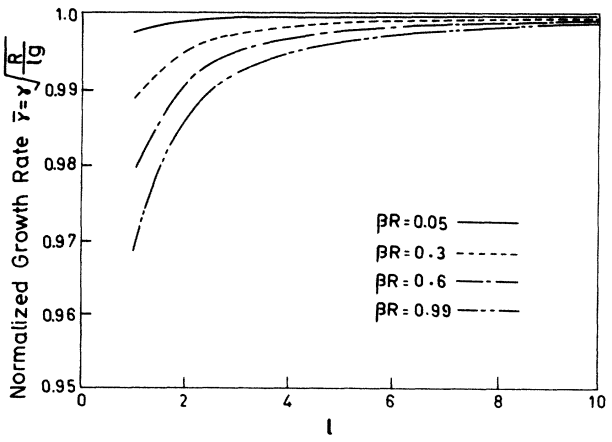

FIG. 1. The normalized growth rate $\bar\gamma$ as a function of l for various values of βR.

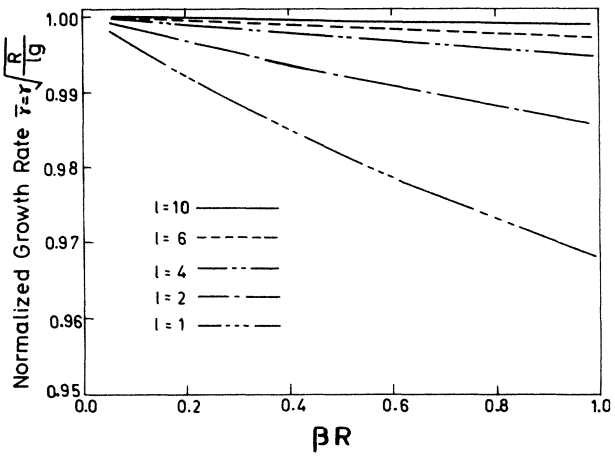

FIG. 2. The normalized growth rate $\bar{\gamma}$ as a function of βR for various values of l.

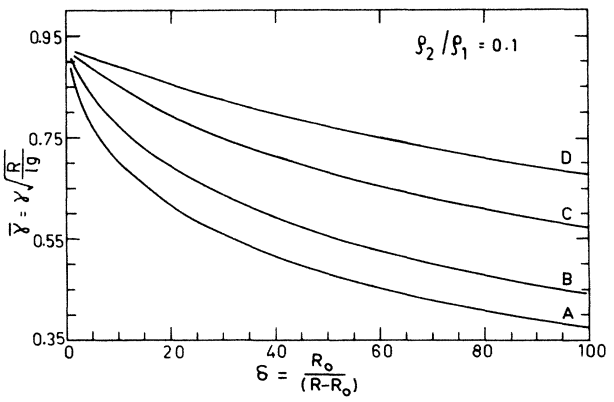

FIG. 3. The normalized growth rate $\bar{\gamma}$ as a function of the aspect ratio δ for various values of l with a density ratio $\rho_2/\rho_1=0.1$. Curves $A-D$ correspond to $l=1,2,5,10$, respectively.

constant $a\to l+1$ and hence in the limit of $\beta R\to 0$ Eq. (15) gives $\bar{\gamma}^2=1$. This is as expected because this limit corresponds to a constant plasma density profile.

An approximate expression for the growth rate is obtained by retaining only the first dominating term in the expansion for ${}_1F_1$ and reads as

$$\bar{\gamma}^2=\frac{2(l+1)\{[(2l+1)^2-\beta^2R^2+2\beta R]^{1/2}-1\}}{(2l+1)^2-\beta^2R^2+2\beta R-1}\ . \tag{17}$$

We have solved Eq. (15) numerically for the positive root $\bar{\gamma}^2$ by retaining up to 10 terms in the hypergeometric series. It is observed that for an accuracy of up to five significant digits two, or at the most three, terms in the series are sufficient for low values of βR ($\beta R\sim 0.5$) while for large values of βR ($\beta R\sim 1$) five to six terms are required for the same accuracy. Figure 1 shows the numerically evaluated growth rate $\bar{\gamma}$ as a function of l for four different values of βR. It is seen from the figure that, for a given value of βR, as l increases $\bar{\gamma}$ increases approaching unity for a very large value of l in agreement with the analytical predictions. In Fig. 2 we have plotted $\bar{\gamma}$ against the parameter βR for five representative values of l. We observe that for a given value of l the growth rate $\bar{\gamma}$ decreases (from its value of unity for $\beta R=0$) as βR increases. However, the variations of $\bar{\gamma}$ with βR (l) for a given value of l (βR) are generally small.

Next, consider a shell of constant density ρ_1 with inner radius R_0 and the outer radius R surrounded by an ablating plasma of constant density ρ_2 extending from $r=R$ to infinity. In this case, the solution of Eq. (6) with the free-surface boundary condition at $r=R_0$ yields the following quadratic equation for the growth rate γ^2:

$$\left[\frac{l}{l+1}+\nu\xi^{-(2l+1)}\right]\bar{\gamma}^4+\left\{\left[1+\frac{l+1}{l}\xi^{-(2l+1)}\right]\nu+[1-\nu\xi^{-(2l+1)}]\xi\right\}\bar{\gamma}^2+\frac{l+1}{l}\xi\nu[1-\xi^{-(2l+1)}]=0\ , \tag{18}$$

where $\xi=R/R_0=(\delta+1)/\delta$, δ being, the aspect ratio of the shell, and the quantity ν is defined as

$$\nu=\frac{l(\rho_2-\rho_1)}{(l+1)\rho_1+l\rho_2}\ . \tag{19}$$

The positive root of Eq. (18) is the required growth rate of the instability. It is easy to verify that as $R_0\to 0$, the solution of Eq. (18) yields for the growth rate expression (11), corresponding to the case of the solid sphere. Further in the limit of infinitesimally thin shells $\xi\to 1$, the instability growth rate $\gamma\to 0$, while the other stable root $\to -(l+1)/l$. It is also interesting to note that in the short wavelength limit ($l\gg 1$), Eq. (18) implies that $\bar{\gamma}^2=(\rho_1-\rho_2)/(\rho_1+\rho_2)$, which is the same as the Atwood number. In general, the normalized growth rate $\bar{\gamma}$ depends on the aspect ratio δ and the plasma density ratio ρ_2/ρ_1. The behavior of the growth rate $\bar{\gamma}$, with respect to the aspect ratio δ, is shown in Figs. 3 and 4. The curves A to D in these figures correspond to values $l=1$, $l=2$, $l=5$, and $l=10$, respectively. The density ratio $\rho_2/\rho_1=0.1$ and 0.01 for the curves in Figs. 3 and 4,

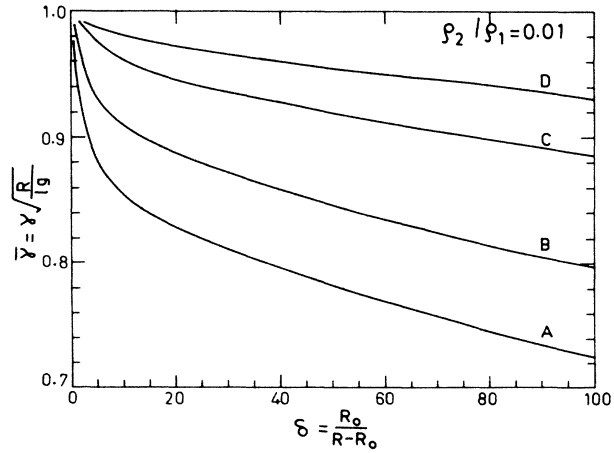

FIG. 4. Same as Fig. 3 but for the density ratio $\rho_2/\rho_1=0.01$.

respectively. We observe from these figures that for a given value of l the growth rate $\bar{\gamma}$ decreases as the aspect ratio δ increases. Further, for a given δ the growth rate $\bar{\gamma}$ asymptotically approaches the classical value of $(\rho_1-\rho_2)/(\rho_1+\rho_2)$ for the large value of l, as noted earlier. Also note that the variation of the growth rate $\bar{\gamma}$ with δ is much slower for higher harmonics. This implies that shell targets with high aspect ratios are more sensitive to short wavelength perturbations.

The analysis of this paper can be generalized to study the effects of a more realistic density profile generated when a ICF pellet is ablated by a laser beam. In particular, the effects due to density steepening may be evaluated by approximately treating the density profile as a combination of step functions and exponentials.

[1]J. H. Nuckolls, L. Wood, A. Thiessen, and G. Zimmerman, Nature **239**, 139 (1972).
[2]G. I. Taylor, Proc. R. Soc. London Ser. A **201**, 192 (1950).
[3]S. Chandrasekhar, *Hydrodynamic and Hydromagnetic Stability* (Oxford University, London, 1968).
[4]R. G. Evans, A. J. Bennett, and G. J. Pert, Phys. Rev. Lett. **49**, 1639 (1982).
[5]D. B. Henderson and R. L. Morse, Phys. Rev. Lett. **32**, 355 (1974).
[6]J. N. Shiau, E. B. Goldman, and C. I. Weng, Phys. Rev. Lett. **32**, 352 (1974).
[7]M. H. Emery, J. H. Gardner, and J. P. Boris, Phys. Rev. Lett. **48**, 667 (1982).
[8]R. L. McCrory, L. Montierth, R. L. Morse, and C. P. Verdon, Phys. Rev. Lett. **46**, 336 (1981).
[9]J. D. Lindl and W. C. Mead, Phys. Rev. Lett. **34**, 1273 (1975).
[10]J. R. Freeman, M. J. Clauser, and S. L. Thompson, Nucl. Fusion **17**, 223 (1977).
[11]T. Yabe and K. Niu, J. Phys. Soc. Jpn. **40**, 1164 (1976).
[12]R. L. McCrory, R. L. Morse, and K. A. Taggert, Nucl. Sci. Eng. **64**, 163 (1977).
[13]C. P. Verdon *et al.*, Phys. Fluids **25**, 1653 (1982).
[14]W. Manheimer, D. Colombant, and E. Ott, Phys. Fluids **27**, 2164 (1984).
[15]K. O. Mikaelian and J. D. Lindl, Phys. Rev. A **29**, 290 (1984).
[16]D. G. Colombant and W. M. Manheimer, Phys. Fluids **26**, 3127 (1983).
[17]N. K. Gupta and S. V. Lawande, Plasma Phys. Controlled Fusion (to be published).
[18]S. E. Bodner, Phys. Rev. Lett. **33**, 761 (1974).
[19]L. Baker, Phys. Fluids **26**, 627 (1983).
[20]H. Takabe and K. Mima, J. Phys. Soc. Jpn. **48**, 1793 (1980).
[21]J. N. Hunt, Appl. Sci. Res. Sect. A **10**, 59 (1961).
[22]L. A. Elliot, Proc. R. Soc. London Ser. A **284**, 397 (1965).
[23]R. E. Kidder, Nucl. Fusion **16**, 3 (1976).
[24]D. L. Book and I. B. Bernstein, J. Plasma Phys. **23**, 521 (1980).
[25]H. Takabe, L. Montierth, and R. L. Morse, Phys. Fluids **26**, 2299 (1983).
[26]G. M. Murphy, *Ordinary Differential Equations and Their Solutions* (Van Nostrand, New York, 1960).